THEORY OF OPTICAL ELLIPSOMETRIC MEASUREMENTS FROM MUSCLE DIFFRACTION STUDIES

Y. YEH AND R. J. BASKIN
Departments of Applied Science and Zoology and Graduate Group in Biophysics, University of California, Davis, California 95616

ABSTRACT A theory of optical ellipsometry describing the complete phase shift and ellipticity of light diffracted from a single muscle fiber is developed. We show that both the phase shift information, described commonly by the birefringence of the fiber, and the ellipticity information, described by the differential polarizability ratio, are necessary to provide a complete picture of the complex contributions to the total optical anisotropy spectra from a diffraction pattern derived from the striated muscle cell. Both form and intrinsic contributions play significant roles in either the birefringence measurement or the differential field ratio measurement. However, we show that their relative weights in these two measured quantities are different, and measuring both of these parameters is necessary to obtain a more complete assessment of the cross-bridge structure and dynamics. The theoretical results have been tested for three different situations: solvent index matching, passive stretch of a resting fiber, and cross-bridge changes under isometric conditions. Comparisons between experimental data and simple model calculations provide much information regarding cross-bridge orientation and structure.

INTRODUCTION

Electromagnetic techniques of investigation have always played an important role in probing the structure and dynamics of molecules. As the molecular system under investigation becomes more complex, the techniques which are most useful have been those which can more specifically describe detailed aspects of the complex system with little interference from less specific parts. Time-resolved x-ray diffraction has provided detailed information about muscle structure at the cross-bridge level (Huxley and Kress, 1985). Spin and fluorescent probe experiments have also yielded structural and dynamic information about cross-bridge motion (Morales et al., 1982; Barnett et al., 1986; Cooke et al., 1982). However, being extrinsic probes, the interpretations of these results require detailed attention and caution as to the actual probe orientation vs. cross-bridge orientation (Ajtai and Burghardt, 1987) and possible probe perturbation of fiber activation (Titus et al., 1987). The optical diffraction method has played a major role in providing information at the sarcomere level, but its role as a significant intrinsic probe of the cross-bridge mechanism is hampered by the long optical wavelength. Historically, transmission birefringence has been used often to characterize the change in fiber anisotropy during muscle contraction (Eberstein and Rosenfalck, 1963; Taylor, 1975; Baylor and Oetliker, 1977). A resurgence of this activity is evidenced by the very recent work of Carlson et al. (1987) and Irving et al. (1987). Our group has conducted research on monitoring the polarization properties of light on the various orders of muscle fiber diffraction pattern (Yeh et al., 1983; Baskin et al., 1986). In this paper, we have combined the two intrinsic optical wavelength probes, birefringence and diffraction, to show that a good deal of specificity exists with respect to cross-bridge structure assignment in this combined technique of investigation. We shall provide a detailed analysis of the method, pointing out what specific molecular information can be obtained and where some ambiguities in data interpretation still remain.

Conceptually, diffraction ellipsometry has some important differences from transmission birefringence. We shall examine these distinctions throughout this work. Muscle fibers are highly ordered in their molecular arrangement; accordingly, there exists a complex mixture of factors contributing to the observed data. The main theme of this paper will be to provide the theoretical framework to elicit structural information from these spectra in an unambiguous fashion. We have recently described the theoretical framework for our experiments qualitatively (Yeh et al., 1985). In the present paper, we will examine the theory behind this experimental technique in a more quantitative fashion. Specifically, we shall investigate in detail the ability of this method to quantitatively ascertain the contributions of form and intrinsic anisotropy to the total optical polarization spectrum derived from diffraction by muscle fibers.

Conceptual Difference between Diffraction Ellipsometry and Birefringence

Both experiments, transmission birefringence and diffraction ellipsometry, measure the state of polarization of the

light after the source of light has encountered scattering elements, in this case, the muscle fiber. In the birefringence experiment, only the phase difference between the two polarization components is measured. In the diffraction ellipsometry experiment, it is the light scattered into a particular diffraction order alone that is collected. To see the differences in these two measurements, we argue in the following manner. In both cases we are dealing with the coherent field contributions. Thus the total field amplitude vectors are the result of vector additions, leading to a resultant amplitude and a net phase for each of the two field components. In Fig. 1, we have sketched the resultant vectors for the two experimental cases. Each of the secondary vectors derived from the interaction has a finite amplitude and a fixed phase angle relative to the previous vector. When these secondary vectors of infinitesimal amplitudes are summed end to end, the spirals of Fig. 1 are formed. The distance from the first vector to the tip of the last vector is the resultant vector. In the case of the forward transmission experiment, the vector sum corresponds to the end-to-end addition of the secondary vectors and the noninteracting forward vector (Fig. 1). Because the forward noninteracting vector is typically much larger than the secondary vectors, the birefringence experiment measures the relative angle of the two long vectors; that angle is defined as the phase shift in a birefringence experiment. Note that due to the large amplitude of the noninteracting contribution, the difference between the magnitudes of the two resultant vectors, $\mathbf{E}_{xo}$ and $\mathbf{E}_{yo}$, normally cannot be discerned. On the other hand, if we remove the long noninteracting vector contribution from each of the total vectors, then the new vectors resulting from the sum of only secondary vectors, $\mathbf{E}_{xd}$ and $\mathbf{E}_{yd}$, form the defining elliptical polarization phase shift on the diffraction maximum. At the same time, however, the dissimilar magnitudes between these two field components are much more discernible due to the absence of the large forward noninteracting signal. Thus, the advantage of the diffraction ellipsometry experiment over that of the forward birefringence experiment is that both parts of the information necessary to fully characterize the elliptically polarized light can be unambiguously obtained. What remains to be shown is why is it necessary to determine both parts.

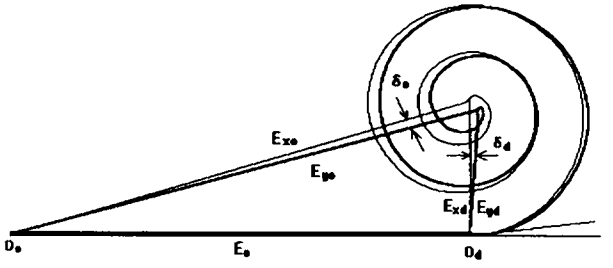

FIGURE 1 Representations of the resulting vectors for forward birefringence and diffraction birefringence. For the forward signal, each of the resultant field components, $\mathbf{E}_{xo}$ and $\mathbf{E}_{yo}$, has a strong noninteracting $\mathbf{E}_o$ summed into it. On the diffraction order, there is no forward contribution, thus one has only the vector sums resulting in $\mathbf{E}_{xd}$ and $\mathbf{E}_{yd}$. Note that here the magnitude differential is accentuated in comparison with the forward birefringence measurement. However, the phase shifts, δ_o and δ_d, are very similar in values.

Consider the simplest case of an optically isotropic, transparent plate which is being stress-modulated along one of the transverse directions. This mechanical modulation provides a density modulation along that direction of the plate and the induced polarizability correspondingly differs from that of the unstressed direction. Generally this is a very small amplitude modulation, and the amplitudes of $\mathbf{E}_x$ and $\mathbf{E}_y$ differ only by a small amount. When combined with the forward noninteracting beam, the small amplitude changes are not discernible. On the other hand, the small E-field difference also reflects on the dielectric constants, ϵ_x and ϵ_y. Each of the electric field components normal to the plate now experiences different effective wavelengths, λ_x and λ_y. The corresponding phase shift between $\mathbf{E}_x$ and $\mathbf{E}_y$ is indeed discernible when the material traversed is substantially thick. Thus the small stress perturbation can be completely characterized in a forward birefringence experiment. There is essentially no need to conduct an independent scattering experiment at all.

Consider next a randomly oriented distribution of intrinsically anisotropic molecules in an optically isotropic medium. These molecules are assumed to have polarizability anisotropy but no permanent dipole moments. The forward birefringence experiment can measure this anisotropy if light traverses a measurable solution path. However, often, as in the case of a solution of myosin rods, without external field alignment there is very little intrinsic solution birefringence (Highsmith and Eden, 1985). On the other hand, if one examines the scattering of light at a nonforward direction, the small molecular anisotropy can be discerned by conducting a depolarized light scattering experiment because there is no longer the presence of the noninteracting forward beam (Highsmith et al., 1982). Thus information about the small degree of intrinsic anisotropy of these molecules can be obtained from such scattering experiments.

In these two cases, we have provided situations where either the phase or the amplitudes can provide the complete necessary information for the characterization of the material system. There is basically only one set of unknowns and that can be obtained by either of the experiments. Generally, we choose the simpler of the two methods. For the muscle fiber, however, there are at least two general classes of optical anisotropy: form, brought about by the extraordinarily regular arrangement of the protein material within the cell, and intrinsic, characteristic of those specific molecular elements that are intrinsically optically anisotropic. There are, then, two sets of unknowns: form anisotropy and intrinsic anisotropy. Each of the experiments described above in principle provides two independent observables, phase and amplitude differ-

entials, and thus, when both observables are used, is self-sufficient for the unraveling of the two pieces of information needed. However, the forward birefringence experiment is at a severe disadvantage in that the small difference in the amplitudes of the two field components is not easy to discern due to the inevitability of noise associated with the presence of the strong noninteracting forward beam (Fig. 1). We provide in this paper a discussion of the combined contributions of form and intrinsic parts to the diffraction ellipsometry.

THEORY

1. The Form Contribution

The arrangement of totally optically isotropic elements in ordered fashion affects the electromagnetic field vectors. If we consider just a single dielectric ellipsoid of dielectric constant ϵ_2, in a medium equally isotropic but with dielectric constant ϵ_1, the electric field lines within the ellipsoid will differ from that external to the ellipsoid due to polarization effects of the dielectric. This is a classical problem which appears in, among other places, Stratton's Electromagnetic Theory (1941). Bragg and Pippard (1953) used this result as the starting point of their analysis of form birefringence. Briefly, the field along direction i within the dielectric ellipsoid which has its major axis aligned along the incident field direction, E_{oi}, is given by

$$E_i = \frac{E_{oi}}{1 + \left(\frac{\epsilon_2 - \epsilon_1}{\epsilon_1}\right) L_i} \tag{1}$$

the factor L_i is the corresponding shape depolarization factor. Note that for an ellipsoid of revolution, L_i has two distinct values, $L_\parallel$ and $L_\perp$, and accordingly, the effective field within the dielectric differs depending on the field orientation with respect to the axes of the ellipsoid. We have used a subscript i to denote $\parallel$ and $\perp$ directions. Because the applied field within the dielectric induces a polarization field, the effective dielectric constant, ϵ_i, correspondingly is affected. For a single ellipsoid of revolution in the medium of ϵ_i, we have

$$\epsilon_i = \epsilon_1 + \frac{f_o(\epsilon_2 - \epsilon_1)}{1 + \left(\frac{\epsilon_2 - \epsilon_1}{\epsilon_1}\right) L_i} \tag{2}$$

where f_o is the volume fraction of total space occupied by this single ellipsoid.

If now there is a number of these dielectric elliposoids of revolution all arranged in the same orientation, and they occupy a total volume fraction f of the total space, then the field outside any particular dielectric ellipsoid is affected by the presence of other dielectric ellipsoids. This is the Lorentz-Lorenz effect. Applying the condition that the external field, E_{oi}, must equal the total field outside and inside the ellipsoids, we have: $E_{oi} = fE_i + (1 - f)F_i$, where F_i is the effective applied field outside the dielectric ellipsoids, and E_i is the field within these ellipsoids. From this relationship, we can show that

$$F_i = \frac{1 + \left(\frac{\epsilon_2 - \epsilon_1}{\epsilon_1}\right) L_i}{1 + (1 - f)\left(\frac{\epsilon_2 - \epsilon_1}{\epsilon_1}\right) L_i} E_{oi}. \tag{3}$$

Substituting Eq. 3 into Eq. 1 and letting E_{oi} of Eq. 1 be replaced by F_i, the resulting field inside the ellipsoid, E_i, now takes on the form

$$E_i = \frac{E_{io}}{1 + kL_i}, \tag{4}$$

where $k = (1 - f)\ [(\epsilon_2 - \epsilon_1)/\epsilon_1]$. Correspondingly, the effective dielectric constant along direction i is given by

$$\epsilon_i = \epsilon_1 + \frac{f(\epsilon_2 - \epsilon_1)}{1 + kL_i}. \tag{5}$$

Even though these expressions were derived by considering a sparse distribution of elements, Bragg and Pippard showed that indeed the equations, here Eqs. 4 and 5, are good approximations even for rather dense arrays.

We can next develop the form contributions to both quantities: birefringence and differential field ratio (DFR).

a. Form Birefringence. This type of birefringence is the result of a difference in the dielectric constant in the two directions, $i = \{\parallel, \perp\}$, as a result of shapes and arrangements of dielectric materials. We define the birefringence due to the form effect alone as $\Delta\epsilon_F$, given by the difference between the dielectric constants along the parallel and perpendicular directions of this dielectric ellipsoid. This is given by

$$\Delta\epsilon_F = \epsilon_\parallel - \epsilon_\perp = f(\epsilon_2 - \epsilon_1)\left(\frac{1}{1 + kL_\parallel} - \frac{1}{1 + kL_\perp}\right). \tag{6}$$

To examine analytically the significance of this form effect, we consider the simple case where $kL_i \ll 1$. Thus all terms of $(kL_i)^2$ and higher can be safely ignored. We have

$$\Delta\epsilon_F \sim fk(\epsilon_2 - \epsilon_1)\,(L_\perp - L_\parallel)\,[1 - k(L_\perp + L_\parallel)]. \tag{7}$$

Note that the leading term is directly proportional to three factors: (*a*) the volume fraction f occupied by the dielectric material, (*b*) the difference of the depolarization coefficients, and (*c*) the difference in the dielectric constants between the dielectric and the surrounding medium. An analysis of the magnetic depolarization coefficients by Stoner (1945) can be carried over completely to the electric depolarization case. Bragg and Pippard listed a few of the values obtained by Stoner in their work. The table compiled by Stoner, giving L_i values vs. μ, where $\mu = b/a$ is the ratio of the minor to major axes of the ellipsoid of revolution, has been converted into a figure (Fig. 2). It can

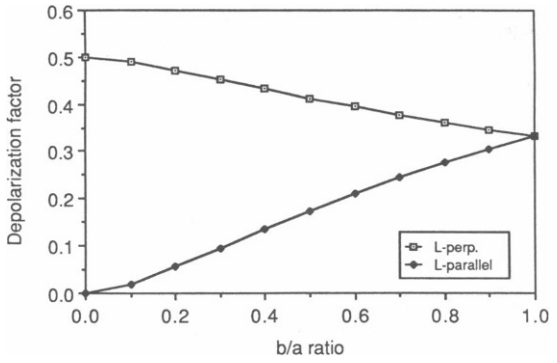

FIGURE 2 Shape depolarization factors, L_i, for prolate ellipsoids whose semi-major axis is aligned along the field direction. $L_\perp$ (□) and $L_\parallel$ (♦). Data from Stoner (1945).

be seen that the basic form birefringence for prolate ellipsoids is always positive, because $L_\perp > L_\parallel$.[1]

b. Form Differential Field Ratio (DFR), r_F. Recall that the effective electric field values at any point inside the ellipsoid are given by Eq. 4. Because the response field of the dielectric is basically the induced electric dipole field produced by that effective electric field, the amplitude of that emitted radiation field is proportional to the product of the field strength, E_i, and the magnitude of the dielectric constant (Eq. 5) minus that of the solvent. Thus,

$$(E_{dip})_i = M(\epsilon_i - \epsilon_l) E_i, \tag{8}$$

where M is the coefficient related to the strength of the electric dipole emission. In the forward direction, the total field is the sum of this dipole field and that of the unscattered E_{oi}. Thus we write

$$(E_{tot})_i = E_{oi} + (E_{dip})_i. \tag{9}$$

We can next define the differential ratio to represent the difference in the fields along the two directions of polarization normalized by the sum of the same two quantities. This will be called DFR in this paper, and mathematically given the symbol of r. Since we are dealing with the form effect alone here, we have r_F. For the forward direction we have

$$(r_F)_o = \frac{(E_{tot})_\parallel - (E_{tot})_\perp}{(E_{tot})_\parallel + (E_{tot})_\perp}. \tag{10}$$

The subscript o denotes forward direction. If we now impose the condition that $E_{o\parallel} = E_{o\perp} = E_o$, then upon substituting Eqs. 8 and 9 into Eq. 10 with the appropriate Eqs. 4 and 5, we get

$$(r_F)_0 = \frac{Mf(\epsilon_2 - \epsilon_1)\left[\frac{1}{(1 + kL_\parallel)^2} - \frac{1}{(1 + kL_\perp)^2}\right]}{2 + Mf(\epsilon_2 - \epsilon_1)\left[\frac{1}{(1 + kL_\parallel)^2} + \frac{1}{(1 + kL_\perp)^2}\right]} \tag{11}$$

Using the same set of approximations as we did for Eq. 7, we have

$$(r_F)_o \approx Mfk(\epsilon_2 - \epsilon_1)\Delta L \cdot \{1 - Mf(\epsilon_2 - \epsilon_1)[1 + k(L_\perp + L_\parallel)]\}, \tag{12}$$

where $\Delta L = L_\perp - L_\parallel$ is used. Note that indeed r_F and $\Delta\epsilon_F$ are directly related, and for the cases of concern here, long cylindrical rods, $r_F > 0$; we have positive DFR as well as positive form birefringence. The magnitude of this DFR quantity is small due to the presence of the factor M.

If the DFR value were measured off the forward direction, then

$$(r_F)_s = \frac{(E_{dip})_\parallel - (E_{dip})_\perp}{(E_{dip})_\parallel + (E_{dip})_\perp}, \tag{13}$$

which upon reduction becomes

$$(r_F)_s \approx k\Delta L \tag{14}$$

Here, the subscript s denotes scattered light alone. Note that there is no longer the factor of M to reduce the magnitude of this contribution. However, the volume fraction dependence of the two expressions, Eqs. 12 and 14, is different. For the nonforward direction, r_F is proportional to $(1 - f)$, whereas r_F for the forward direction is proportional to $f(1 - f)$.

2. The Intrinsic Contribution

We next consider strictly intrinsic contribution without any form effect. Thus we are considering point anisotropic dipoles of very dilute concentration in some solvent. Assuming that the solvent medium has a dielectric constant ϵ_l, then the effective principal dielectric constants along each of the direction i, for the elemental region of intrinsically anisotropic matter are given by

$$\epsilon_i^{(o)} = \epsilon_l + \epsilon_i', \tag{15}$$

where $\epsilon_i^{(o)}$ is the diagonal dielectric tensor element along direction i, $i = \{\parallel, \perp\}$. ϵ_i' is the difference between the value of the intrinsic anisotropic dielectric constant along the ith direction and that of the isotropic surrounding medium. The intrinsic birefringence is then

$$\Delta\epsilon_{IN} = \epsilon_\parallel^{(o)} - \epsilon_\perp^{(o)} = \epsilon_\parallel' - \epsilon_\perp'. \tag{16}$$

Assuming that the anisotropic molecules will experience the full extent of the external field, E_{oi}, the induced dipole will have a field strength given by $(E_{dip}) = M \cdot \epsilon_i' \cdot E_{oi}$, and according to our definition, Eq. 10, the DFR for the

[1]Birefringence is normally defined as $\Delta n = n_\parallel - n_\perp$. However for nonmagnetic materials, $n^2 = \epsilon$. Thus $\epsilon_\parallel - \epsilon_\perp = n_\parallel^2 - n_\perp^2 = (n_\parallel - n_\perp)(n_\parallel + n_\perp) \sim 2\bar{n}\Delta n$. Consequently, $\Delta\epsilon$ is related to Δn by the constant $2\bar{n}$. We shall use $\Delta\epsilon$ in the theoretical development and transform to Δn when we compare theoretical results with the experimental data in the next section of this paper.

intrinsically anisotropic elements in the forward direction becomes

$$(r_{IN})_o = \frac{M(\epsilon_\parallel' - \epsilon_\perp')}{2 + M(2\epsilon_1 + \epsilon_\parallel' + \epsilon_\perp')}. \tag{17}$$

If M is a small quantity, we then have

$$(r_{IN})_o \approx \frac{M}{2}(\epsilon_\parallel' - \epsilon_\perp'). \tag{18}$$

The nonforward DFR value is once again obtained by not including the noninteracting component. Thus we have

$$(r_{IN})_s \approx \frac{\epsilon_\parallel' - \epsilon_\perp'}{2\epsilon_1}\left(1 - \frac{\epsilon_\parallel' + \epsilon_\perp'}{2\epsilon_1}\right), \tag{19}$$

which is still very small, although certainly larger than the forward effect. This is the basis for conducting scattering experiments away from the forward direction if one wants to measure small differences in polarization field magnitudes. We see also from Eqs. 16 and 19 that either measurement is adequate for the complete characterization of the intrinsic anisotropy of molecules.

3. The Combined Effect

For a system exhibiting both form and intrinsic contributions, the local field effects on E_i and the dielectric constants must be considered. The two defining equations are now the altered E-field expression,

$$E_i = \frac{E_{oi}}{1 + k_i L_i} \tag{20}$$

and the altered dielectric function expression

$$\epsilon_{mi} = \epsilon_1 + \frac{f_m(\epsilon_{mi}^{(o)} - \epsilon_1)}{1 + k_{mi} L_{mi}}. \tag{21}$$

We note that here the partial volume fraction, f_m, where $m = \{A, I\}$, represents the region of the fiber under consideration. Note also that the previous constant, k, has now both spatial and directional specificity.

$$k_{mi} = (1 - f_m)\left(\frac{(\epsilon_{mi}^{(o)} - \epsilon_1)}{\epsilon_1}\right), \tag{22}$$

where $\epsilon_{mi}^{(o)}$ is the intrinsic dielectric function in region m of the fiber along direction i. The same regional identification applies for the depolarization factor, L_{mi}.

In this study of the muscle fiber where intrinsic and form anisotropies are coupled, we must again make a distinction between the forward and the diffraction order experiment. From our previous work on the diffraction intensity from muscle fibers (Yeh et al., 1980), we used the electric dipole scattering expression as the starting point for the diffraction analysis. That equation is (Berne and Pecora, 1976)

$$\mathbf{E}_{sc} \propto \exp(ik_s r_o) \int_v d^3 r e^{i\mathbf{q}\cdot\mathbf{r}}\, \delta\epsilon(\mathbf{r}) \cdot \mathbf{E}_o(\mathbf{r}). \tag{23}$$

Here, r_o is the distance from the fiber to the detector and $\mathbf{q} = \mathbf{k}_s - \mathbf{k}_o$ is the difference wavevector between the incident wavevector $\mathbf{k}_o$ and the scattered wavevector $\mathbf{k}_s$. We note first of all that it is the spatial fluctuations of the dielectric constant, $\delta\epsilon(\mathbf{r})$ that will lead to scattering. Because this dielectric constant is a tensor quantity, the polarization of scattered field can differ from the polarization of the incident field. The principal eigen-elements of this tensor for a fiber system with cylindrical symmetry are given by Eq. 21, where the index i indicates parallel or perpendicular directions to the fiber axis. The applied field $\mathbf{E}_o$ of Eq. 23 must further be corrected for local field effects so the electric field at the scattering point should be that given by Eq. 20.

The spatial periodicity of the sarcomere and subsarcomeric length elements constitutes a periodic grating with departure of the dielectric constant from that of the solvent medium given by its spatial Fourier components:

$$\delta\epsilon(\mathbf{r}) = \sum_j \exp(-i[j\mathbf{K}\cdot\mathbf{r}])\,\delta\epsilon_j, \tag{24}$$

where the order of the Fourier component is indexed by j, and $|\mathbf{K}| = (2\pi)/D$, D being the sarcomere length. Using the principal coordinates, and upon substituting Eq. 24 into Eq. 23 we obtain

$$(\mathbf{E}_{sc})_i \propto e^{ik_s r_o} \sum_j \int_v d^3 r e^{i[\mathbf{q}-j\mathbf{K}]\cdot\mathbf{r}} (\delta\epsilon_j)_i \mathbf{E}_i. \tag{25}$$

The specific direction for detecting the coherent diffraction process can be obtained by an evaluation of the integral, which in the limiting case is a sharp Dirac δ-function at each of the diffraction orders ($\mathbf{q} = j\mathbf{K}$). We note further that the specific order of the dielectric constant enters in two significant places of Eq. 25. It enters as a response function $(\delta\epsilon_j)_i$ of the fiber elements to the effective field, and it also enters as a phase factor in the propagating wave given by $\exp(i\mathbf{k}_{si} r_o)$.

Consider the phase factor first. The quantity $\mathbf{k}_{si}$ is the wavevector of the scattered field with the polarization plane along i, and can be written as

$$\mathbf{k}_{si} = \mathbf{k}_{so}\sqrt{\epsilon_i}, \tag{26}$$

where $\mathbf{k}_{so}$ is the wave vector in vacuum. The presence of the medium, which includes both the solvent and the muscle fiber, is represented by the total dielectric constant. The dielectric constant in Eq. 26 must include contributions from both the fiber and the bathing medium. Thus, we have

$$\epsilon_i = \epsilon_1 + (\delta\epsilon_j)_i, \tag{27}$$

and one sees that the zeroth order dielectric constant differs from the jth order by the different values of the jth Fourier component ($j = 0, 1, 2, \ldots$).

We next consider the diffraction amplitudes. According to Eq. 25, the diffraction amplitude of the jth order is

proportional only to the jth order dielectric constant or the polarizability of the medium. This fact is a restatement of Eq. 8 here for the case of the dielectric grating. Thus, an anisotropic dielectric grating will affect both the phase and the amplitude of the diffracted wave. To carry out such an analysis, we need to use a model system which exhibits an anisotropic index or refraction or dielectric grating. For simplicity, we use the following model.

There will be two regions of the I-band bordering a symmetrically located A-band within each period of the sarcomere. The averaged intrinsic dielectric constant of the A-band, $\bar{\epsilon}_A^{(o)}$, will be assumed to be larger than that of the I-band dielectric constant, $\epsilon_I^{(o)}$. Furthermore, the A-band dielectric constant is assumed to be intrinsically anisotropic, thus, $\bar{\epsilon}_A^{(o)} = (\epsilon_{A\parallel}^{(o)} + \epsilon_{A\perp}^{(o)})/2$, whereas the I-band is assumed to be intrinsically isotropic. Fig. 3 depicts the model to be used for the remainder of this study.

The result of Fourier decomposition of this spatial grating is given by

$$(\delta\epsilon_o)_i \rightleftharpoons \epsilon_{i0} = \frac{2}{D}\left[\epsilon_{Ii}\left(\frac{D}{2} - z_A\right) + \epsilon_{Ai} z_A\right] \tag{28}$$

$$(\delta\epsilon_j)_i \rightleftharpoons \epsilon_{ij} = \frac{1}{j\pi}(\epsilon_{Ai} - \epsilon_{Ii}) \sin(jKz_A), \tag{29}$$

where $2z_A$ is the A-band length and j is the order of diffraction maximum.

a. Zeroth Order Birefringence. Eq. 28 can now be applied to each of the two polarization orientations. The birefringence experienced by the zeroth order signal is given by

$$(\Delta\epsilon)_o = \epsilon_{\parallel o} - \epsilon_{\perp o} = \frac{2}{D}\left[\left(\frac{D}{2} - z_A\right)(\epsilon_{I\parallel} - \epsilon_{I\perp}) + z_A(\epsilon_{A\parallel} - \epsilon_{A\perp})\right], \tag{30}$$

where $\epsilon_{A\parallel}$, $\epsilon_{I\parallel}$, $\epsilon_{A\perp}$, and $\epsilon_{I\perp}$ will each include both form and intrinsic parts according to the appropriate Eq. 21. We have, upon substitution,

$$(\Delta\epsilon)_o = \frac{2}{D}\left\{\left(\frac{D}{2} - z_A\right) f_I \Delta\epsilon_I^{(o)}\left(\frac{1}{1 + k_{I\parallel}L_{I\parallel}} - \frac{1}{1 + k_{I\perp}L_{I\perp}}\right) + z_A f_A\left[\frac{\Delta\epsilon_{A\parallel}^{(o)}}{1 + k_{A\parallel}L_{A\parallel}} - \frac{\Delta\epsilon_{A\perp}^{(o)}}{1 + k_{A\perp}L_{A\perp}}\right]\right\}, \tag{31}$$

where $\Delta\epsilon_I^{(o)} = (\epsilon_I^{(o)} - \epsilon_I)$, $\epsilon_{A\parallel}^{(o)} - \epsilon_I = \Delta\epsilon_{A\parallel}^{(o)}$, and $\epsilon_{A\perp}^{(o)} - \epsilon_I = \Delta\epsilon_{A\perp}^{(o)}$. If each of the components of kL is small, (<0.1 in value) and the differences in the $\parallel$ and $\perp$ components of kL is negligible, then Eq. 31 reduces to an approximate form given by

$$(\Delta\epsilon)_o \approx \frac{2}{D}\left[\left(\frac{D}{2} - z_A\right) f_I k_I \Delta\epsilon_I^{(o)} \Delta L_I + z_A f_A \bar{k}_A \Delta\bar{\epsilon}_A^{(o)} \Delta L_A + z_A f_A(\epsilon_{A\parallel}^{(o)} - \epsilon_{A\perp}^{(o)})\right] \tag{32}$$

Here, we have used the fact that $\Delta\bar{\epsilon}_A^{(o)} = (\epsilon_{A\parallel}^{(o)} + \epsilon_{A\perp}^{(o)})/2 - \epsilon_I$ and $\bar{k}_A = (k_{A\parallel} + k_{A\perp})/2$. We note that this expression is the weighted sum of the birefringence from both the A-band and the I-band regions. Indeed if the dielectric constant of the solvent medium is matched out, $\Delta\epsilon_I^{(o)} = \Delta\bar{\epsilon}_A^{(o)} = 0$, only the intrinsically anisotropic part remains. But note that for banded indices or for intrinsically anisotropic elements, there is never a point where the form effect can be rigorously matched because of the different values of ϵ_I that will be needed for such a match.

b. First Order ($j = 1$) Birefringence. Because the dielectric constant experienced by the field is the combined zeroth order and first order parts, we need to add the two contributions to obtain the total dielectric constant. Thus, using Eq. 29, the first diffraction order birefringence due to the first Fourier dielectric component is given by

$$(\Delta\epsilon)_1 = \frac{1}{\pi}\sin(Kz_A)\,[(\epsilon_{A\parallel} - \epsilon_{A\perp}) - (\epsilon_{I\parallel} - \epsilon_{I\perp})]. \tag{33}$$

Upon substitution of the appropriate Eq. 21, we have

$$(\Delta\epsilon)_1 = \frac{1}{\pi}\sin(Kz_A)\left[f_A\left(\frac{\Delta\epsilon_{A\parallel}^{(o)}}{1 + k_{A\parallel}L_{A\parallel}} - \frac{\Delta\epsilon_{A\perp}^{(o)}}{1 + k_{A\perp}L_{A\perp}}\right) - f_I\Delta\epsilon_I^{(o)}\left(\frac{1}{1 + k_{I\parallel}L_{I\parallel}} - \frac{1}{1 + k_{I\perp}L_{I\perp}}\right)\right]. \tag{34}$$

In the same limit of small kL for each of the components, we have the approximate expression.

$$(\Delta\epsilon)_1 = \frac{1}{\pi}\sin(Kz_A) \cdot [f_A\bar{k}_A\Delta\bar{\epsilon}_A^{(o)}\Delta L_A - f_I k_I \Delta\epsilon_I^{(o)}\Delta L_I + f_A(\epsilon_{A\parallel}^{(o)} - \epsilon_{A\perp}^{(o)})], \tag{35}$$

where the approximations $\bar{\epsilon}_{A\parallel}^{(o)} \approx \bar{\epsilon}_{A\perp}^{(o)} \approx \bar{\epsilon}_A^{(o)}$ and $k_{A\parallel} \approx k_{A\perp} \approx \bar{k}_A$ are used. This part is to be added to the zeroth order part in order to have an expression for the total diffraction birefringence. So the total first order birefrin-

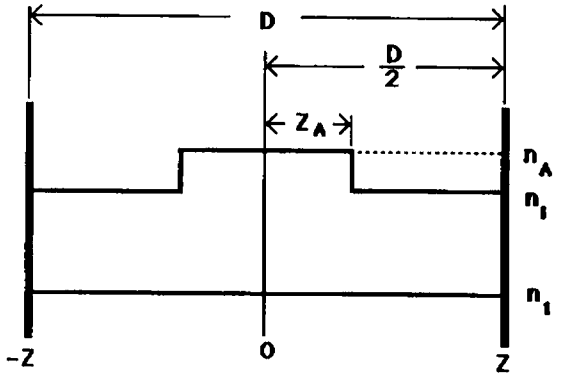

FIGURE 3 Model of simplified sarcomere unit with appropriate indices of refractions indicated. The values of n_I for the solvent and n_I for the I-band are assumed to be isotropic, whereas n_A can assume two values, $n_{A\parallel}$ and $n_{A\perp}$. The sarcomere length is defined as D, whereas the A-band length is given by $2z_A$.

gence is given by

$$(\Delta\epsilon_T)_1 = (\Delta\epsilon)_o + (\Delta\epsilon)_1 \tag{36}$$

c. First Order Differential Field Ratio (DFR). The DFR on the diffracted order will be defined by the two polarization orientations. However, for the essence of this analysis, we have arbitrarily set the diffraction angle related to the diffracted order to unity.

$$r_T \equiv \frac{(E_{diff})_\parallel - (E_{diff})_\perp}{(E_{diff})_\parallel + (E_{diff})_\perp}. \tag{37}$$

The field components, $(E_{diff})_i$ will be given by the product of the first order dielectric function and the local field given by Eq. 20. We must consider that the mass density of the A-band and the I-band are in fact different. From our previous discussion, this feature is incorporated in the expression for the form contributions where the volume fractions of the A- and I-regions are now different. These values are represented by f_A and f_I, respectively. For the local dielectric constant, we have used the specific form-adjusted volume fractions. For the local fields, however, we have taken an averaged local field across the A- and I-band. We considered this approximate field to be a reasonable one because of the smallness of the differential dielectric constants between the A-I bands. Consistent with this approximation, we write

$$r_T = \frac{(\epsilon_{A\parallel} - \epsilon_{I\parallel})\dfrac{E_o}{1 + \bar{k}L_\parallel} - (\epsilon_{A\perp} - \epsilon_{I\perp})\dfrac{E_o}{1 + \bar{k}L_\perp}}{(\epsilon_{A\parallel} - \epsilon_{I\parallel})\dfrac{E_o}{1 + \bar{k}L_\parallel} + (\epsilon_{A\perp} - \epsilon_{I\perp})\dfrac{E_o}{1 + \bar{k}L_\perp}}, \tag{38}$$

where ϵ_{mI} is the first order differential dielectric constant given by Eq. 21 and $\bar{k} \approx (\bar{k}_A + k_I)/2$. The new expression for DFR, upon substituting the appropriate Eq. 20, is given by

$$r_T \approx \frac{f_A\Delta\epsilon^{(o)} + f_A\bar{k}_A\,\Delta\bar{\epsilon}_A^{(o)}\,\Delta L_A - f_I k_I\,\Delta\epsilon_I^{(o)}\,\Delta L_I}{2(f_A\,\Delta\bar{\epsilon}_A^{(o)} - f_I\,\epsilon_I^{(o)})}. \tag{39}$$

Note the very interesting denominator in the above expression. If the volume fractions of the A- and I-regions are identical, $f_A = f_I = f$, then the denominator becomes $2f\Delta\epsilon_{AI} = f(\epsilon_{A\parallel}^{(o)} + \epsilon_{A\perp}^{(o)} - 2\epsilon_I)$. This quantity is very much smaller than the denominator of any of the other DFR expressions that we have obtained so far. The reason for this effective amplification of the DFR value is because the diffraction signal is a particular scattering signal which exists only because there is an A-I differential. Because generally the differential dielectric constant between the $\parallel$ and the $\perp$ components of A-band is much smaller than the differential dielectric constants between the averaged A-band and I-band regions, the last two terms of the numerator can be combined to give $fk\Delta L\,(\Delta\epsilon_{AI})$. That is the same as the factor in the denominator. Dividing each term of the numerator and denominator by $2f\Delta\epsilon_{AI}$, we have

$$r_T \approx r_o + \frac{\bar{k}\Delta L}{2} \tag{40}$$

with r_o given by

$$r_o \equiv \frac{\epsilon_{A\parallel}^{(o)} - \epsilon_{A\perp}^{(o)}}{2\Delta\epsilon_{AI}}. \tag{41}$$

Note that the intrinsic part is not divided by the dielectric differential between material and medium, but rather scaled by the dielectric differential between the A-band and the I-band. Although this latter differential is large when compared with the intrinsic differential dielectric constants, it is still very small compared with the matter-medium dielectric differential, $\Delta\bar{\epsilon}$. Thus, by conducting the experiment on the diffraction order instead of conducting an off-diffraction measurement or a forward measurement, we can, in this limit of equal volume fractions, gain an enhancement in the visibility of the intrinsic contribution of r_T by the ratio $\Delta\bar{\epsilon}/\Delta\epsilon_{AI}$. The form contribution, on the other hand, is not correspondingly enhanced. This favorable amplification of the intrinsic anisotropy component allows the measurement of both the form and intrinsic contributions of anisotropy in a fiber system.

Returning once more to the expression where the volume fractions are realistically not identical, $f_A \neq f_I$, the impact of this inequality is that the value of DFR is suppressed by the amount of this ratio, f_I/f_A. We summarize the results of this section by defining

$$\begin{aligned} F_I &\equiv f_I\Delta\epsilon_I^{(o)}k_I\,\Delta L_I \\ F_A &\equiv f_A\Delta\bar{\epsilon}_A^{(o)}\bar{k}_A\Delta L_A, \end{aligned} \tag{42}$$

where these F_m factors are strictly from form effects, and defining

$$\Delta\epsilon^{(o)} \equiv \epsilon_{A\parallel}^{(o)} - \epsilon_{A\perp}^{(o)}, \tag{43}$$

as the A-band intrinsic effect. In these terms, the total birefringence and total DFR will yield the following equations:

$$(\Delta\epsilon_T)_1 = F_I + \left(R_A + \frac{1}{\pi}\sin\pi R_A\right)[(F_A - F_I) + f_A\Delta\epsilon^{(o)}] \tag{44}$$

$$(r_T)_1 = \frac{(F_A - F_I) + f_A\Delta\epsilon^{(o)}}{2(f_A\Delta\bar{\epsilon}_A^{(o)} - f_I\Delta\epsilon_I^{(o)})}, \tag{45}$$

where $R_A = (2z_A)/D$. In these two equations, even though form and intrinsic parts of the diffraction ellipsometric signal appear to be in identical form in one of the factors, the form part also appears in a different way so that these equations are in fact linearly independent. Thus in principle, an inversion of the two equations will allow for the unique determination of the form and intrinsic contributions. In the next section, we shall discuss some of the modeling studies of a fiber system where both parts

contribute. For changes in the form contribution, either the volume fraction or the shape factor will be affected, while for intrinsic changes, only values of the anisotropy factors along and perpendicular to the field directions will be affected.

RESULTS AND DISCUSSION

The results of the theoretical section will be applied to several cases. We will use the over-simplified model of Fig. 3 so that the physical principles can be clearly illustrated. As a preface of such an analysis based on Eqs. 44 and 45, an approximate treatment of the overlap and nonoverlap regions of the A-band must be considered. From the model described in Fig. 3, there are but two regions of the sarcomere under consideration. The A-band region and a part of the I-band that does not overlap with the A-band. However, it is clear that at any particular sarcomere length, there is a region of the fixed A-band that overlaps into the region of the I-band. Such an overlap is important on two accounts. First, the cross-bridges that are coming into contact with the overlapping I-band may be situated differently from those outside the overlap region. Second, the indices of the overlap region may be different from either the A-band or the I-band regions. In our simplified model, we consider only part one of these two problems. That is, we consider only how the cross-bridge elements are going to affect the optical properties of the polarized light on the diffraction order. The insertion of more assumed isotropic I-band element into the overlap region will, to first approximation, change the intensity distribution of the orders, and only secondarily change the polarization properties of diffracted light in a form birefringence change. Accordingly, for the balance of this discussion, we shall not consider that part.

Because the amount of overlap is a function of the sarcomere length, the A-band will be divided into two parts: nonoverlap and overlap regions. From Fig. 3, it is clear that if both the I-band length, z_I, and A-band length, z_A, are constants, then the nonoverlap region (NOL) of the A-band is given by

$$\mathrm{NOL} = \frac{D}{2} - z_I, \tag{46}$$

where D is the sarcomere length. The two parts of the A-band will be specified as the nonoverlap region, normalized by z_A to give $\rho \equiv \mathrm{NOL}/z_A$, and the overlap region, $1 - \rho$.

Within this A-band, there will be the contributions from both S-1 and S-2 to the optical properties on the diffraction order. S-1 will be assumed to be optically isotropic due to its more globular nature. Thus S-1 will only contribute via the form anisotropy aspect. More specifically, as S-1 moves out towards the thin filament, its averaged projection will make the effective ellipsoid of the A-band less prolate, thus decreasing ΔL_A. It is clear that this decrease of form anisotropy will only come from that part of the A-band that is within the overlap. Thus, the effective shape change, $(\Delta L_A)_{\mathrm{eff}}$, due to S-1 movement in a radial sense will be given by

$$(\Delta L_A)_{\mathrm{eff}} = (1 - \rho)(\Delta L_A)_{\mathrm{OL}} + \rho(\Delta L_A)_{\mathrm{NOL}}, \tag{47}$$

where

$$(\Delta L_A)_i = (L_{A\perp} - L_{A\parallel})_i = 1 - \frac{3}{2} m \frac{s p_i}{z_A}. \tag{48}$$

Here, p_i is the portion of the empty space between the A-band and the I-band that is now assumed to be occupied by the projecting S-1 elements, and m is the assumed constant slope of the ΔL_A vs. μ plot (Fig. 2). We have defined μ_i = minor axis/major axis = $(sp_i)/z_A$, with s as the lattice spacing between the A-band and the I-band. The subscript i denotes either the overlap region or the nonoverlap region. The extent that the S-1 heads move from a position near that of that myosin rod towards the actin filament is governed by the values of p_i. For the relaxed fiber, the extension of S-1 may be, on the average, a small portion of the total spacing s when within the overlap region. On the other hand, p_i for the nonoverlap region may be either larger or smaller than that in the overlap region. We shall examine both of these two cases.

Both S-2 and LMM are assumed to be optically anisotropic in an uniaxial sense with respect to light in the visible wavelength (633 nm). We have previously discussed the change of the optical anisotropy upon the tilt of the intrinsically anisotropic element, S-2. In that analysis, the myosin rod is assumed to have intrinsic anisotropy parameters, ϵ_o and ϵ_e, where the subscripts o and e refer to the ordinary and extraordinary polarization axes. The existence of this distinct o and e dielectric constants is the first requisite for intrinsic anisotropy of a substance. If now the myosin rod is assumed to be able to bend at the LMM-S-2 hinge region, the anisotropy will be altered due to the different projection of optically anisotropic element presented to the incident light. In our previous analysis (Yeh and Baskin, 1987), the thick filament *sans* S-1 was considered as being composed of axially symmetrically arranged tilted anisotropic rods with the portion of the tilted region given by p_o. The resulting principal anisotropic dielectric tensor is given by

$$\bar{\epsilon} = \begin{bmatrix} \epsilon_\perp & 0 & 0 \\ 0 & \epsilon_\parallel & 0 \\ 0 & 0 & \epsilon_\perp \end{bmatrix} \tag{49}$$

where

$$\epsilon_\parallel = [2\epsilon_o X + \epsilon_o(1 - 2X)]p_o + \epsilon_e(1 - p_o) \tag{50a}$$

$$\epsilon_\perp = [\epsilon_o(1 - X) + \epsilon_e X]p_o + \epsilon_o(1 - p_o). \tag{50b}$$

The tilt angle θ_t, of the S-2 region is related to the factor X

by the relationship

$$X = \frac{\sin^2 \theta_t}{2}. \tag{51}$$

In considering that within the A-band, there are the two regions corresponding to overlap and nonoverlap of the I-band, we must again arrive at an averaged angle of tilt. This is most simply approximated by

$$\Delta\epsilon_{\text{eff}}^{(o)} = (1 - \rho)\Delta\epsilon_{\text{OL}}^{(o)} + \rho\Delta\epsilon_{\text{NOL}}^{(o)}, \tag{52}$$

where the notations are as previously defined.

As is with the case of S-1, the orientational angle of the S-2 part of myosin may be different when the filaments are within overlap in comparison with the nonoverlap case. Here, we will have two values of X, corresponding to the two tilt angles. Again, the tilt angle with nonoverlap may be larger or smaller than the tilt angle with overlap. These two situations will be further analyzed in the test cases.

Having defined the effective shape change of the A-band and the effective intrinsic anisotropy due to the regional tilting of the S-2 elements, we are now in a position to insert the quantities of $(\Delta L_A)_{\text{eff}}$ and $(\Delta\epsilon^{(o)})_{\text{eff}}$ into the equations for an analysis of the trends in ellipsometry changes. The total birefringence given in terms of the dielectric constants in Eq. 40 is converted to index of refraction by the use of footnote 1, where $\bar{n} = (\bar{n}_A + n_1)/2$ is assumed. Here $\bar{n}_A = (n_o + n_e)/2$.

1. Choice of Numerical Constants in the Model Calculations

To carry out the model calculations, three sets of parameters have to be specified. These are the lattice dimensions, the index of refraction values, and the volume fractions.

a. Lattice Parameters. A distinction is made between the intact fiber and the skinned fiber. In particular, when the fiber is stretched, the change in the lattice spacing between the skinned and that of the intact is different. For the case of the intact fiber, we have assumed that there is total isovolumic nature of the fiber system (Matsubara and Elliot, 1976). Given a unit volume at a given sarcomere length, stretch of the fiber will be at the expense of the transverse lattice dimension, s, so that the volume is kept constant. Thus the transverse lattice value is given by

$$s = (V_o/(\pi D))^{1/2}, \tag{54}$$

where the constant volume V_o is defined at some referenced sarcomere length.

The skinned fiber lattice values are obtained from the functional relationships measured experimentally by Higuchi and Umazume (1986) for chemically skinned fibers. This system is not isovolumic, but it is also not a system where the lattice parameter is independent of the sarcomere length. A nearly quadratic decrease of s is quite prominent in their data. We fitted their data to a curve described by the equation

$$s = s_o - \beta(D - D_o)^2, \tag{50}$$

where the value of $\beta = 0.004(\mu\text{m})^{-1}$ was the best fit number to the data. The value of s_o is assumed to be larger than the corresponding intact fiber value of s_o at the same sarcomere length by ~10%. This choice is dictated by the fact that upon the perforation of the membrane structure, we have observed such an overall swelling of the fiber lattice at constant D (Baskin, J., unpublished data). The values of D_o and s_o used here are $D_o = 2.2$ μm, $s_o = 0.037$ μm.

b. Index of Refraction Parameters. In our model calculation, we need three indices of refraction besides the one for the solvent medium. The assignment of indices of refraction for the extraordinary and ordinary rays of the A-band medium and another isotropic index of refraction for the I-band constitutes the minimum required. This problem is difficult because there is no direct method of experimentally obtaining these values. Taylor (1975) has used for pure proteins, an index of refraction of nearly 1.57. However, this value is obtained without a full consideration of the hydration of the protein, which decreases the averaged index of refraction at the rather large visible wavelengths. Indeed, Bragg and Pippard used a value of 1.53 for hydrated proteins in their estimates. Fujime and Yoshino (1978) have related the effective index of refraction to the density of the medium. This is correct for a relative differential measure, but the proportional factor is in fact the microscopic polarizability, and that value is not available. Because our model requires explicit assignment of the values, not simply the differentials, we could not use them. Ellipsometry has been used to measure the index of refraction of monolayers of proteins deposited onto substrates (Arwin, 1985). However, the values of the index obtained depends on the nature of the substrate, which can denature the proteins and thus pack them in denser layer with an index nearer to that of 1.57. Indeed, in his study, different proteins acquire different values on the same substrate, pointing to the differential denaturation and anisotropy of the protein systems in general. Without a consistent basis to rely upon a particular set of values, we set upon to use our ellipsometer and directly measure the change in birefringence upon index matching. The *ansatz* for this experiment is that we can use the matching studies to obtain the total form matching point. There, the averaged index of all protein medium is matched as well as can be given that there is banded intrinsic anisotropy. We will then assign values of the A-I differential indices and the intrinsic anisotropies to fit the experimental data at that point.

For this study, n_1 is varied from the value of pure water, ($n_1 = 1.334$) to that of the averaged protein material, the form contribution decreases and comes to a minimum at the total matching condition. The experimental study was conducted with great care to minimize the effect of the

index-matching fluid on the integrity of the fiber molecular elements. Simply placing a relaxed fiber in typical index matching fluids such as *O*-toluidine (Colby, 1971) causes irreversible changes in the ellipsometry data. That is, upon the resubstitution of the matching fluid by the normal interstitial fluid, the ellipsometry parameters of the fiber do not revert to their original values. Our procedure, then, is to first place the resting skinned fiber in the rigor state at pH = 7.0. Then, the fiber is successively fixed with gluteraldehyde and osmium tetroxide, exactly as if we were going to examine the fiber under the electron microscope. At this stage, several index-matching fluids were tried. Any fluid which led to irreversible change in either Δn_T or r_T was discarded along with the fiber. New fixed fibers were again prepared. We found that sucrose did not affect the integrity of the fiber in this fixed state adversely as judged by the almost complete reversibility of r_T. On the other hand, the process of fixation did dramatically alter the state of the fiber from that of the original fiber (relaxed state), and this is presented in Table I. We see that even though birefringence did increase by ~20% from the rigor state value upon chemical action in the fixation process, the DFR changed significantly more during the stages of the fixation: relax, rigor, rigor-fix. This observation is a strong reinforcement of our notion that the intrinsic contribution affects the value of measured DFR differently from that of total birefringence. Furthermore, we cannot say that the DFR value obtained in the fixed fiber is a true representation of the nonfixed fiber.

For the actual experiments, sucrose was allowed to come to equilibrium before data was taken. This process usually took 2 h at each of the high sucrose concentrations. Data presented in Fig. 4 show that indeed Δn_T decreases upon increasing match of the indices between the fiber and the solution. At the same time, the values of r_T in these fixed fibers also decreased in magnitudes upon an increase in sucrose concentration. We emphasize that the actual values of either total birefringence or total DFR cannot be considered the realistic values of the fiber because of the fixation process. However, the use of this procedure to reach a point of solution index of refraction match with the fiber is reasonable. Our data shows that we cannot get a complete match with 60% wt/wt sucrose (n_l = 1.4419). However, the observed trends are very clear. A quadratic fit to the birefringence data can be extrapolated to show

TABLE I
CHANGE OF TOTAL BIREFRINGENCE Δn_T AND TOTAL DFR, r_T, UPON THE FIXATION PROCEDURE BEFORE IMBIBING IN INDEX MATCHING SOLUTIONS FOR A REPRESENTATIVE SINGLE SKINNED FIBER (R 6.1.#1.2)

Condition of fiber	Δn_T	r_T	SL
In relaxing solution	$1.21 \pm 0.02 \times 10^{-3}$	0.051 ± 0.008	2.52
Rigor state	$1.36 \pm 0.02 \times 10^{-3}$	0.040 ± 0.004	2.38
Fixed state	$1.61 \pm 0.03 \times 10^{-3}$	0.025 ± 0.005	2.40

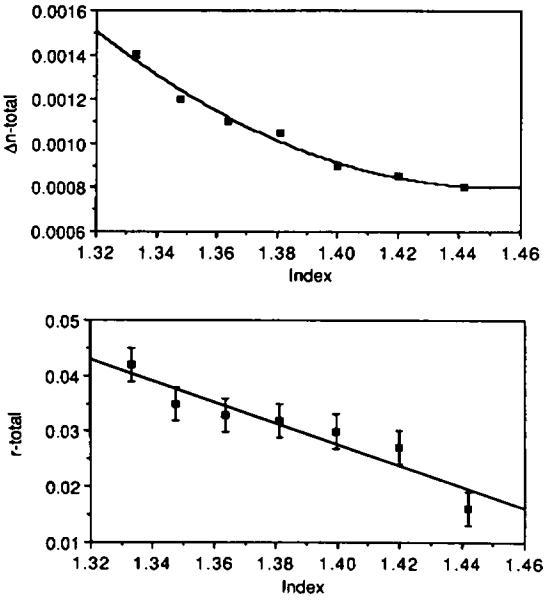

FIGURE 4 Experimental results of Δn-total (*a*) and *r*-total (*b*) vs. index of refraction change brought about by changes in the concentration of sucrose in aqueous medium. Data show that there is a leveling out of Δn_T near 1.46. This result indicates that the effective index of refraction of the fiber elements in the sarcomere configuration is substantially lower than 1.57, that of pure protein material.

that form is nearly matched out at an index of refraction of 1.46. We assumed that the match point index of refraction must be nearly that of the lower density I-band, and thus n_I = 1.46 was used. We further used, as the differential index of refraction between these two bands, a value of 0.02, very nearly that of 0.018 measured by Huxley and Niedergerke (1958). Accordingly, the averaged A-band index was assigned the value of $\bar{n}_A$ = 1.48. The A-band intrinsic birefringence values, n_{Ao} and n_{Ae}, were assigned by forcing this index differential so that total birefringence is nearly one-third due to intrinsic and two-thirds due to form contribution, whereas the average value of these two is $\bar{n}_A$. For the remainder of these model calculations, these values of the indices are used: n_{Ae} = 1.483, n_{Ao} = 1.477, n_I = 1.46, n_l = 1.334. These values represent the averaged indices of refraction over domains at least as large as the wavelength of light considering water of hydration.

c. Volume Fractions. The ratio of the material density of the A-band to that of the I-band was measured by Huxley and Hanson (1954) and by Fujime and Yoshino to be nearly 2:1. A somewhat more quantitative estimate can be made using the table in the Appendix section of Bagshaw's Muscle Contraction (1982). Using these values, we estimate that the total weight percentage content of myosin is 5.76% and that of actin is 2.50%. Thus the ratio of myosin to actin is ~2.3:1. Wilke (1968) states that 60% of the proteins in muscle are contractile proteins and the total protein content is 20% of the total muscle weight. Thus 12% by weight may be considered contractile proteins. Assuming the near equivalence of weight percent to a

volume fraction, we have used a total volume fraction of ~12% in these calculations. The breakdown into $f_A = 8.4\%$ and $f_I = 3.6\%$ is based on these considerations. For simulations of adding or reducing mass from the fiber, such as the introduction of cleaved S-1 decorating the actin filament, or the binding of monoclonal antibodies to the S-1 moieties, the corresponding volume fraction is assumed to change in a proportional manner.

2. Test Case Situations

We shall examine several different cases where cross-bridge elements have been modified within the context of this model. We shall analyze the relationship of these imposed modifications to the expected ellipsometry profiles. All of the plots are made with respect to the independent parameter D, the sarcomere length.

a. Purely Form Contribution vs. Total Effect. To model the purely form effect, we impose the condition that n_{Ao} and n_{Ae} both have the values of 1.48. The results for skinned fiber held at a sarcomere length $D = 2.4$ μm are shown in Table II. We note that the purely form contribution is nearly two-thirds of the total birefringence Δn_T. DFR values for the form contribution are a little more than 50% of the total effect when original $f_A = 0.084$ and $f_I = 0.036$ are assumed. The introduction of a more comparable volume fraction leads to a greater enhancement of the DFR value than the corresponding Δn_T. This is consistent with the arguments we presented in the previous section that the intrinsic anisotropy effect can be "amplified" in the DFR given favorable conditions.

b. Skinned Fiber vs. Intact Fiber. The first test is to determine the appropriate orientation of S-2 and the space-filling factor of S-1 in the overlap and nonoverlap regions of a skinned fiber consistent with experimental results. When cross-bridges in the nonoverlap region assume a position along that of the thick filament, then $p_{NOL} = 0.1$ and $(\theta_t)_{NOL} = 0°$. Within the overlap region, we assume that some constraints will govern the overall cross-bridge position. These are stipulated to be $p_{OL} = 0.3$ and $(\theta_t)_{OL} = 10°$. This is case *i* of Fig. 5. The other case in Fig. 5 (*ii*) is where in the nonoverlap region, $p_{NOL} \approx 1.0$ and $(\theta_t)_{NOL} = 45°$. However, in the overlapping region, the values remain as before ($p_{OL} = 0.3$, $(\theta_t)_{OL} = 10°$). We

TABLE II
CALCULATED VALUES OF FORM AND TOTAL CONTRIBUTIONS OF BIREFRINGENCE AND DFR FOR DIFFERENT RATIOS OF f_A AND f_I

f_A	f_I	$\Delta n_F \times 10^3$	$\Delta n_T \times 10^3$	$r_F \times 10^2$	$r_T \times 10^2$
0.084	0.036	0.892	1.219	5.516	8.659
0.075	0.045	0.811	1.103	5.844	9.939
0.065	0.055	0.720	0.973	6.920	14.165
0.060	0.060	0.673	0.907	9.194	23.146

SL = 2.4 μm. $f_T = f_A + f_I = 0.12$ is assumed.

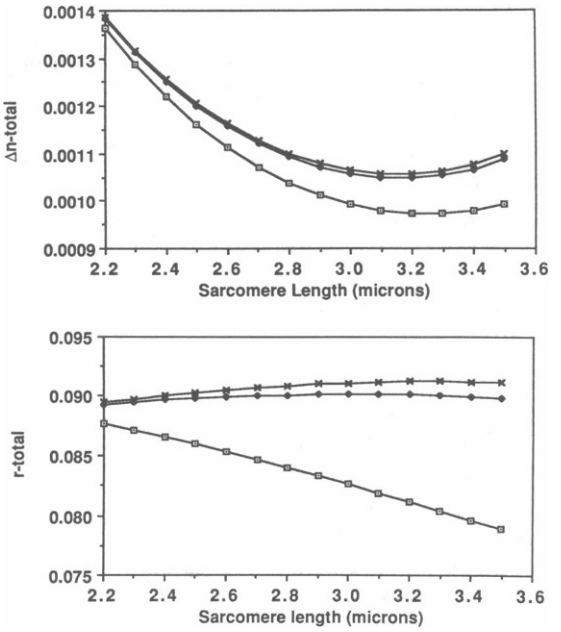

FIGURE 5 Theoretical results of Δn_T and r_T for three different sets of values of p_i and θ_i plotted against sarcomere length, D. (□) $p_{NOL} = 1.0$, $p_{OL} = 0.3$, $\theta_{NOL} = 45°$, $\theta_{OL} = 10°$. (♦) $p_{NOL} = p_{OL} = 0.3$, $\theta_{NOL} = \theta_{OL} = 10°$. (×) $p_{NOL} = 0.1$, $p_{OL} = 0.3$, $\theta_{NOL} = 0°$, $\theta_{OL} = 10°$.

show that these values lead to clearly defined rising and falling trends in both Δn_T and r_T upon sarcomere length increase. A comparison with data from actual experiments on skinned fiber (Fig. 6, *a* and *b*) suggests that our case *ii* is closer to the experimental situation than is case *i*. However, the extent of change is smaller in the model calculation than in actual experiment. Recall that our model comparison is made with the I-band being considered totally isotropic. If this is not the case, one would argue that the

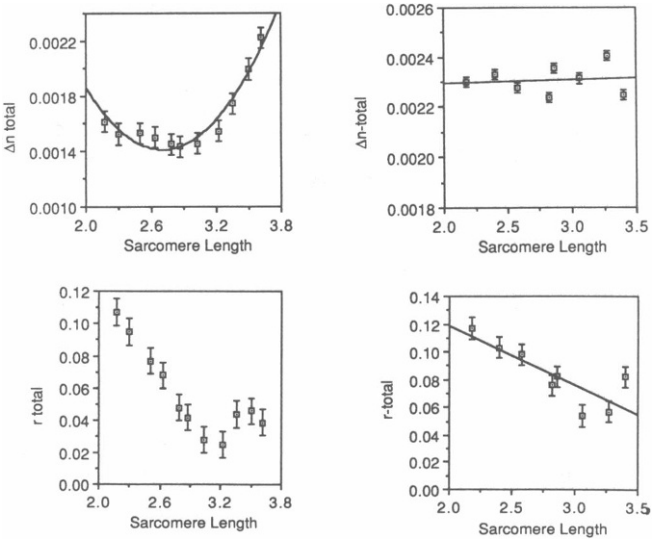

FIGURE 6 Representative experimental data of Δn_T and r_T for passive stretch of fibers in its relaxed state. Both skinned fiber (*a* and *b*) and intact fiber (*c* and *d*) data are shown.

increasing randomness of the nonoverlapping I-bands provides another source of intrinsic anisotropy decrease upon sarcomere length increase. The current theory has not quantitatively incorporated this idea.

For a comparison between skinned and intact fiber, and other subsequent studies, the conditions of case *ii* are imposed. The basic difference between skinned and intact fibers is in the manner of change of the lattice spacing. A change in the lattice spacing will lead to a different volume fraction in the case of skinned fiber. On the other hand, for intact fiber, the isovolumic constraint forces a different packing with essentially no change in either f_A or f_I upon sarcomere length stretch. These results are shown in Fig. 7, *a* and *b*. We note that the total birefringence of the intact fiber is invariably larger than that of the skinned fiber, but as for the DFR, the values are reversed. We also note that the change in either of these quantities upon sarcomere length stretch differs in trend depending on whether the system is skinned or intact. For the intact fiber, because there is no volume fraction change, the observed change is due strictly to changing cross-bridge or lattice configurations. On the other hand, the skinned fiber has additional volume fraction change to be incorporated into the total effects. Experimental data taken on skinned and intact fibers are shown in Fig. 6, *a–b* and *c–d*, respectively, for general qualitative trend comparisons.

c. Modeling Cross-bridge Actions. A key aspect of these studies is to impose prescribed changes in the S-1 and S-2 moieties of the cross-bridge, and to see that the resulting effects are on both the diffraction birefringence and DFR. For control, we have used the skinned fiber data (case *ii*) from the previous studies. Data for the other two potentially attainable situations are given along with the control in Fig. 8, *a* and *b*. First we note that if there is a phase transition which decreases the intrinsic anisotropy of the myosin rod element within the overlapping region (Ueno and Harrington, 1981), and if the lateral cross-bridge movement is assumed to shift but little ($\theta_1 = 45°$, $\theta_2 = 10°$, $p_1 = 1, p_2 = 0.3, n_{A\parallel} = 1.482, n_{A\perp} = 1.478$), then the values of both birefringence and DFR are substantially decreased throughout the sarcomere length stretch. If on the other hand, the most significant cross-bridge action is the tilting up of the S-1 and the corresponding increase of the angle of S-2 within the overlapping region, we have modeled that by an increase in the lateral space occupied by the S-1 and a larger tilt angle for the S-2 elements ($\theta_1 = 45°$, $\theta_2 = 30°$, $p_1 = p_2 = 1.0$, $n_{A\parallel} = 1.483$, $n_{A\perp} = 1.477$). Obviously, this effect diminishes upon sarcomere stretch as the overlap region diminishes. Experimental data for DFR in a skinned fiber undergoing activation is compared with that of the relaxed fiber in Fig. 9. It is seen that the difference between the relaxed and the activated fiber diminishes upon sarcomere length stretch.

d. Altering the S-1 Moieties. We have used three ways to change S-1 content experimentally: chymotrypsin digestion at the S-1 to S-2 hinge, cleaved S-1 decorating the thin filament of a rigor fiber, and introducing monoclonal antibodies specific to S-1. In all three cases signal changes in both the birefringence and DFR are observed. In Fig. 10, *a* and *b*, we illustrate these cases using our model.

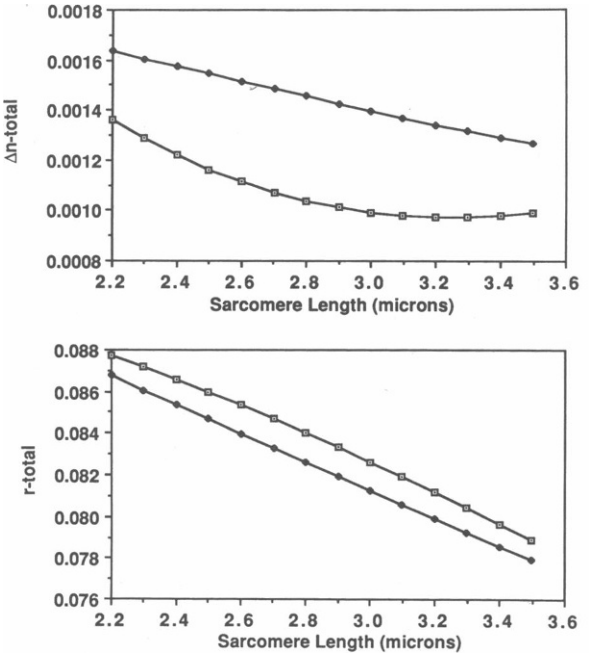

FIGURE 7 Theoretical results of Δn_T and r_T for skinned (□) and intact (♦) fibers. The difference between these curves is due to the difference in the way these fibers change in all three factors: intrinsic anisotropy, lattice parameter, and volume fraction, upon passive stretch.

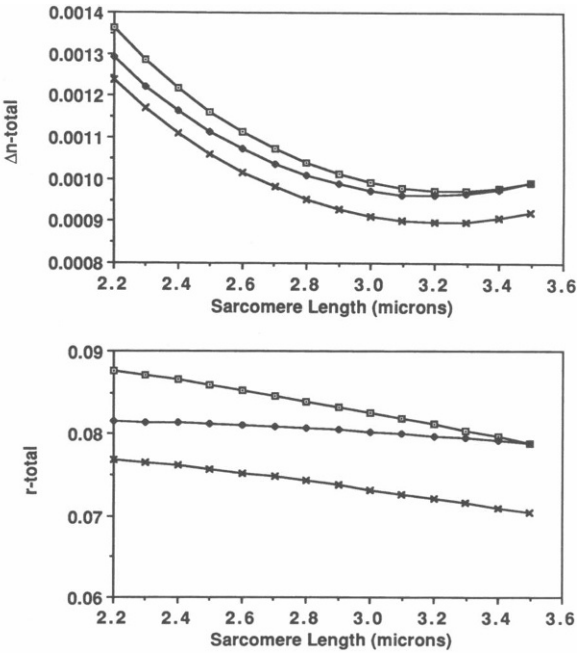

FIGURE 8 Theoretical plots of Δn_T (*a*) and *r*-total (*b*) for three conditions of cross-bridge positions. The reference curves are for the skinned fiber (□) as a control. Data for a molecular phase transition is indicated by (♦). Tilting of S-1 and S-2 without helix melting is shown by (×).

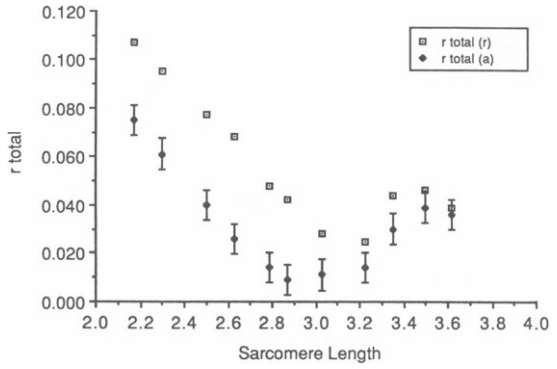

FIGURE 9 Experimental data of r-total upon activation for skinned fiber. Activation data compiled from a number of experiments, each providing one data point. Normalized values are referenced to a single relaxed fiber experiment.

Removing S-1 through chymotryptic digestion leads to a diminished f_A content and gives more freedom to the angle of tilt S-2 ($\theta_1 = 45°$, $\theta_2 = 30°$, $p_1 = 0.1$, $p_2 = 0.1$, $f_A = 0.074$, $f_I = 0.036$). The result is a large decrease in the total birefringence and a significant increase in DFR. The decrease in birefringence has already been reported by us in an earlier work (Baskin et al., 1986) while DFR increase has recently been observed in our laboratory.

Increasing S-1 content on the thin filament increases f_I only. This also restricts the tilt angle in the nonoverlapping region ($\theta_1 = 10°$, $\theta_2 = 10°$, $p_1 = 0.3$, $p_2 = 0.3$, $f_A = 0.084$, $f_I = 0.046$). Using these values, we find that there is a marginal increase in total birefringence while DFR value increased significantly. Parenthetically, the intensity of diffraction signal is decreased as well as the A-I index differential is diminished. We have reported this result recently (Jones et al., 1986).

The introduction of MCA specific to S-1 increases the volume fraction f_A and, to some extent, the space occupied ($\theta_1 = 45°$, $\theta_2 = 10°$, $p_1 = 1.0$, $p_2 = 0.5$, $f_A = 0.09$, $f_I = 0.036$). This leads to an increase in birefringence and a decrease in DFR. Principally, these are form-related effects, and their predictions agree with our experiments (Jones et al., 1987).

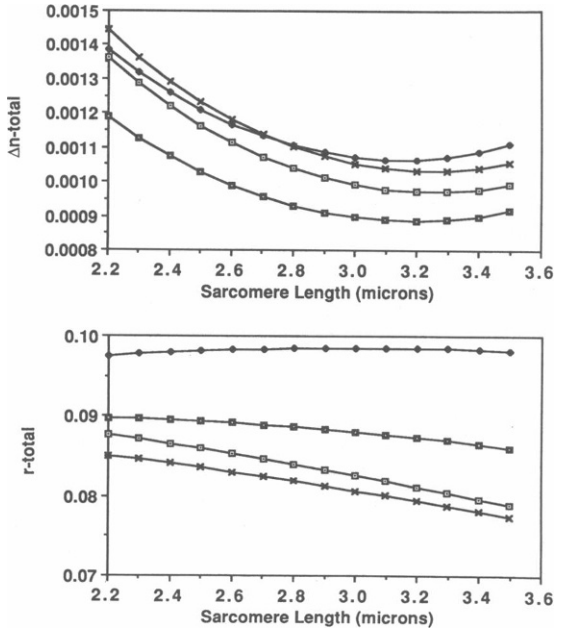

FIGURE 10 Theoretical plots for Δn_T and r_T upon changing volume fractions within the sarcomere. Reference curve (□) is for skinned fiber in assumed relaxed state. Data for the inclusion of decorated f-actin by cleaved S-1 during rigor is given by (♦). When S-1 has been cleaved off the myosin molecules within the fiber and rinsed from the cytoplasm, the data is given by (■). Data for the inclusion of more mass in the A-band due to monoclonal antibodies specific to S-1 is shown by (×).

CONCLUSIONS

We have shown that the optical ellipsometry spectra from the diffraction pattern derived from the muscle fiber is rich in structural information concerning the fiber elements. The full features of the fiber elements cannot be elucidated by measuring either total birefringence or total DFR alone, but requires the measurement of both of these quantities. Such measurements are most readily made on the diffraction orders.

We have also shown that form contribution does indeed contribute a significant part towards both the value of r_T and of Δn_T. However, the weighting of form as compared with the intrinsic part differs in the values of total birefringence and total DFR. Furthermore, by using a very simple model where one considers only A-band material to be optically anisotropic and where the I-band material is isotropic, we have been successful in predicting a majority of the features that have been obtained in experimental situations.

Two significant improvements in the theoretical modeling of the structure and dynamics of the single fiber are needed. The first is the need to refine the role of the S-1 element in its contribution to the form effect. This problem is currently being critically examined by two groups. Irving et al. (1987) has provided experimental evidence to indicate that the form change is a function of the orientation assumed by the S-1 heads. That is to say, our simple assumption that ellipsoids of revolution representing the thick filament should be reexamined so that the individual S-1 orientations can be taken into consideration. Indeed, Carlson et al. (1987) have performed the initial theoretical analysis considering these detailed movements of the S-1 and their effects on the form contribution. The second problem with the current theory as we have presented it is that the I-band has been assumed to be totally isotropic. There are clear indications that this is not rigorously true (Maeda, 1978). In this case, our simplified treatment of the overlap region also needs to be modified. In the study of the diffraction polarization anisotropy recently carried out by Leung and co-worker (Leung and Cheung, 1987; Leung, 1987), the assumption that I-band is indeed anisotropic, albeit less than that of the A-band, has been considered. However, their analysis did not take into

consideration the form contribution. The task remaining is then to refine this model along the directions that have been initiated by these researchers and to quantitatively relate definite features of these experimental spectra to cross-bridge dynamics and structure.

The authors are grateful for the use of unpublished experimental data obtained by their colleagues: J. Baskin, J. S. Chen, H. M. Jones, and S. Shen. The critical reading and discussions of an earlier version of this manuscript by Professor Chen is deeply appreciated.

This work is supported in part by a grant from National Institutes of Health under AR-26817.

Received for publication 8 September 1987 and in final form 11 April 1988.

REFERENCES

Ajtai, K., and T. P. Burghardt. 1987. Microscopic and wavelength dependent fluorescence polarization from 1.5-IAEDANS labeled myosin subfragment 1 decorating muscle fibers in the presence and absence of MgADP. *Biophys. J.* 51:4a.

Arwin, H. 1986. Optical properties of thin layers of bovine serum albumin, γ-globulin, and hemoglobin. *Appl. Spectrosc.* 40:313–318.

Bagshaw, C. R. 1982. Muscle Contraction. Chapman and Hall, London. 30–31, 76.

Barnett, V. A., P. Fajer, C. F. Polnaszek, and D. D. Thomas. 1986. High resolution detection of muscle cross-bridge orientation by electron paramagnetic resonance. *Biophys. J.* 49:144–146.

Baskin, R. J., Y. Yeh, K. Burton, J. S. Chen, and M. Jones. 1986. Optical depolarization changes in single, skinned muscle fibers: evidence for cross-bridge involvement. *Biophys. J.* 50:63–74.

Baylor, S. M., and H. Oetliker. 1977. The optical properties of birefringence signals from single muscle fibres. *J. Physiol. (Lond.).* 264:163–198.

Berne, B., and R. Pecora. 1976. Dynamic Light Scattering. John Wiley & Sons, New York. 33–36.

Bragg, W. L., and A. B. Pippard. 1953. The form birefringence of macromolecules. *Acta Crystallogr.* 6:865–867.

Carlson, F. D., R. C. Haskell, and P. S. Blank. 1987. A model of the form birefringence properties of muscle. *Biophys. J.* 51:471a.

Cooke, R., M. S. Crowder, and D. D. Thomas. 1982. Orientation of spin labels attached to cross-bridges in contracting muscle fibers. *Biophys. J.* 300:776.

Colby, R. H. 1971. Intrinsic birefringence of glycerinated myofibrils. *J. Cell Biol.* 51:763–771.

Eberstein, A., and A. Rosenfalck. 1963. Birefringence of isolated muscle fibres in twitch and tetanus. *Acta Physiol. Scand.* 57:144–166.

Fujime, S., and S. Yoshino. 1978. Optical diffraction study of muscle fibers. I. A theoretical basis. *Biophys. Chem.* 8:305–315.

Highsmith, S., C. C. Wang, K. Zero, R. Pecora, and O. Jardetzky. 1982. Bending motions and internal motions in myosin rod. *Biochemistry.* 21:1182–1187.

Highsmith, S., and D. Eden. 1985. Transient electrical birefringence characterization of heavy meromyosin. *Biochemistry.* 24:4917–4924.

Higuchi, H., and Y. Umazume. 1986. Lattice shrinkage with increasing resting tension of stretched, single skinned fibers of frog muscle. *Biophys. J.* 50:385–389.

Huxley, A. F., and R. Niedergerke. 1958. Measurement of the striations of isolated muscle fibres and the interference microscope. *J. Physiol. (Lond.).* 144:403–425.

Huxley, H. E., and J. Hanson. 1957. Quantitative studies on the structure of cross-striated myofibrils. I. Investigations of interference microscopy. *Biochim. Biophys. Acta.* 23:229–249.

Huxley, H. E., and M. Kress. 1985. Crossbridge behavior during muscle contraction. *J. Muscle Res. Cell Motil.* 6:153–161.

Irving, M., M. Peckham, and M. A. Ferenczi. 1987. Birefringence transients induced by caged-ATP photolysis in demembranated rabbit muscle fibres. *Biophys. J.* 51:3a.

Jones, M., K. Burton, Y. Yeh, and R. J. Baskin. 1986. Depolarization spectrum of diffracted light from skinned fibers: ellipsometry measurements following myosin extraction and HMM labeling. *Biophys. J.* 49:251a.

Jones, M., R. J. Baskin, and Y. Yeh. 1987. Optical analysis of antibody binding to myosin S-1 in muscle fibers. *Biophys. J.* 51:316a.

Leung, A. F. 1987. Degree of polarization of light diffracted from resting striated muscle. *Cell Biophys.* 10:145–168.

Leung, A. F., and M. K. Cheung. 1987. Polarization changes in light diffracted from contracting muscle fibers. *Cell Biophys.* 10:127–144.

Maeda, Y. 1978. Birefringence of oriented thin filaments in the I-bands of crab striated muscle and comparison with the flow birefringence of reconstituted thin filaments. *Eur. J. Biochem.* 90:113–121.

Matsubara, I., and G. F. Elliott. 1972. X-ray diffraction studies on skinned single fibers of frog skeletal muscle. *J. Mol. Biol.* 72:657–669.

Morales, M. F., J. Borejdo, J. Botts, R. Cooke, R. A. Mendelson, and R. Takashi. 1982. Some physical studies of the contractile mechanism in muscle. *Annu. Rev. Phys. Chem.* 32:319–351.

Stoner, E. C. 1945. The demagnetizing factors for ellipsoids. *Philos. Mag.* 36:803–817.

Stratton, J. A. 1941. Electromagnetic Theory. McGraw-Hill Book Co., New York. 213.

Taylor, D. L. 1975. Birefringence changes in vertebrate striated muscle. *J. Supramol. Struct.* 3:181–191.

Titus, M. A., G. Ashiba, and A. G. Szent-Gyorgyi. 1987. The effect of IASL modification on the calcium control of the actomyosin ATPase. *Biophys. J.* 51:28a.

Ueno, H., and W. F. Harrington. 1981. Conformational transition in the myosin hinge upon activation of muscle. *Proc. Natl. Acad. Sci. USA* 78:6101–6105.

Wilke, D. R. 1968. Muscle. Wm. Clowes & Sons Ltd., London. 9–11.

Yeh, Y., R. J. Baskin, R. L. Lieber, and K. P. Roos. 1980. A theory of light diffraction by single skeletal muscle fibers. *Biophys. J.* 29:509–522.

Yeh, Y., M. E. Corcoran, R. J. Baskin, and R. L. Lieber. 1983. Optical depolarization changes on the diffraction pattern in the transition of skinned muscle fibers from relaxed to rigor state. *Biophys. J.* 44:343–351.

Yeh, Y., R. J. Baskin, R. A. Brown, and K. Burton. 1985. Depolarization spectrum of diffracted light from muscle fiber: the intrinsic anisotropy component. *Biophys. J.* 47:739–742.

Yeh, Y., and R. J. Baskin. 1987. Optical ellipsometry studies on the diffracted orders of single fibers from skeletal muscles. *In* Optical Studies of Muscle Cross-bridges. R. J. Baskin and Y. Yeh, editors. CRC Press, Boca Roca, FL 123–148.